

Françoise Damay,^{a*} Adrian Carretero-Genevri^a, Alain Cousson,^a Wouter Van Beek,^b Juan Rodriguez-Carvajal^a and François Fillaux^c

^aLaboratoire Léon Brillouin, CEA-CNRS UMR12, CE Saclay, 91191 Gif sur Yvette CEDEX, France,

^bSwiss–Norwegian Beam Lines at the European Synchrotron Radiation Facility (SNBL at ESRF), Rue Jules Horowitz, 38043 Grenoble CEDEX, France, and ^cLADIR-CNRS, UMR 7075, Université Pierre et Marie Curie, 2 Rue Henry Dunant, 94230 Thiais, France

Correspondence e-mail:
damay@llb.saclay.cea.fr

Synchrotron and neutron diffraction study of 4-methylpyridine-*N*-oxide at low temperature

Received 15 December 2005
Accepted 30 March 2006

The structure of 4-methylpyridine-*N*-oxide has been determined at 250, 100 and 10 K by combined synchrotron (C_6H_7NO) and neutron (C_6D_7NO) powder diffraction experiments. At 250 K the space group is $I4_1/amd$ and the tetragonal unit cell [$a = b = 7.941$ (2), $c = 19.600$ (5) Å] contains eight equivalent molecules. At 100 K the structure is orthorhombic, with space group $Fddd$, $a = 12.138$ (2), $b = 10.237$ (2) and $c = 19.568$ (3) Å. The 16 equivalent molecules are rotated by about 8° around the c axis with respect to positions at high temperature. At 10 K the best structural model corresponds to a tetragonal unit cell with the space group $P4_1$, $a = b = 15.410$ (2) Å and $c = 19.680$ (3) Å. The 32 molecules (eight molecules in the asymmetric unit) show complex reorientations around the three cell axes. Whereas at 250 and 100 K the deuterated methyl groups are largely disordered, at 10 K they are ordered in-phase along infinite chains parallel to **a** and **b**. Face-to-face methyl groups along **c** are in an eclipsed configuration. The structure at 10 K suggests that the manifold of rotational tunnelling transitions could be due to inequivalent lattice sites for crystallographically independent methyl groups.

1. Introduction

Very few studies of the 4-methylpyridine-*N*-oxide (4MPNO, Fig. 1) have been published in the past. This crystal could be, however, an interesting system for experimental studies of non-linear quantum dynamics arising from the collective rotation of methyl groups (Kaiser-Morris *et al.*, 1998), by analogy with the parent compound 4-methylpyridine (4MP). In 4MP the methyl group bound to the pyridine ring can rotate almost freely around the C–C bond, according to the highest ever reported rotational tunnelling frequency at ~ 500 μeV

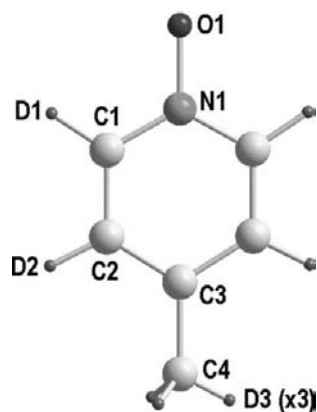


Figure 1
Schematic view of 4-methylpyridine-*N*-oxide.

Table 1
Rigid-body intramolecular distances (Å) and angles (°).

N1—O1	1.347	C1—N1—C1	121.5
N1—C1	1.342	N1—C1—C2	119.4
C1—C2	1.401	C1—C2—C3	122.9
C2—C3	1.386	C2—C3—C4	122.2
C3—C4	1.479	C2—C3—C2	116.0
C1—D1	1.070	N1—C1—D1	117.0
C2—D2	1.090	C1—C2—D2	116.6
C4—D3	0.940 (250 K)	C3—C4—D3	112.3 (250 K)
	0.980 (100 K)		112.9 (100 K)
	1.070 (10 K)		113.0 (10 K)

Table 2
Rietveld refinement of neutron diffraction data for powdered fully deuterated 4-methylpyridine-*N*-oxide at 250, 100 and 10 K.

The standard uncertainty for the last digit is given in parentheses.

Formula	C ₅ D ₄ NO(CD ₃)		
Temperature	250 K	100 K	10 K
Crystal system	Tetragonal	Orthorhombic	Tetragonal
Space group	<i>I</i> 4 ₁ / <i>amd</i> (No. 141)	<i>Fddd</i> (No. 70)	<i>P</i> 4 ₁ (No. 76)
Unit-cell dimensions			
<i>a</i> (Å)	7.941 (2)	12.138 (2)	15.410 (2)
<i>b</i> (Å)	7.941 (2)	10.237 (2)	15.410 (2)
<i>c</i> (Å)	19.600 (5)	19.568 (3)	19.680 (3)
<i>V</i> (Å ³)	1236.0 (6)	2431.4 (8)	4673.6 (10)
<i>Z</i>	8	16	32
Number of reflections	605	1041	8161
Number of parameters	21	28	70
Bragg <i>R</i> -factor	4.62	4.18	4.05
χ ²	2.79	3.74	5.55

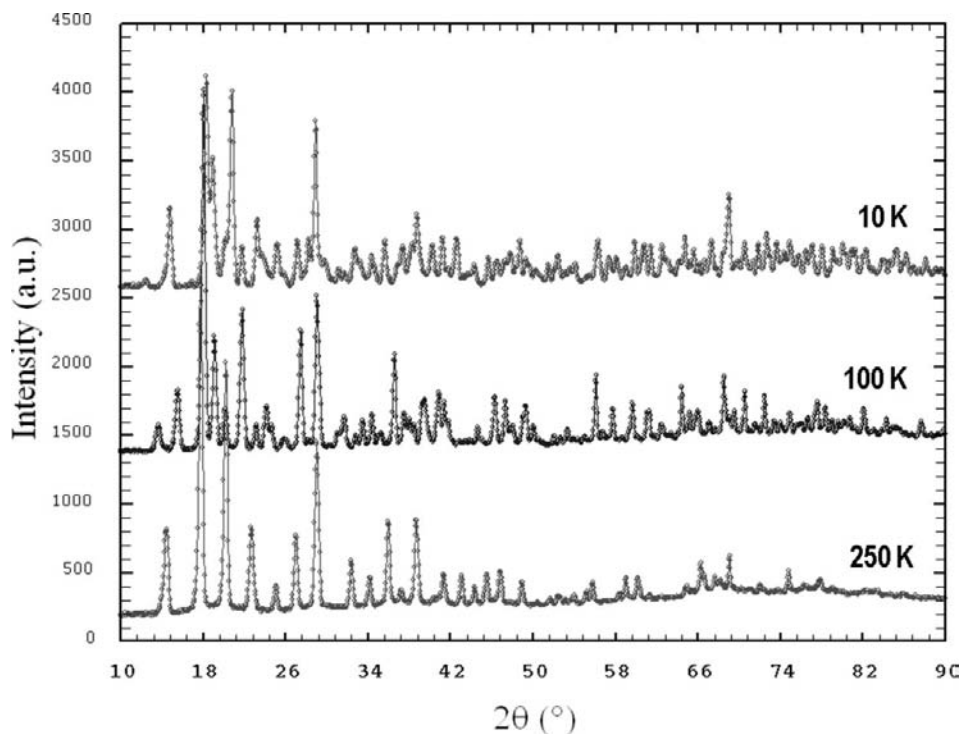


Figure 2
Neutron diffraction patterns of fully deuterated powdered 4-methylpyridine-*N*-oxide at 250, 100 and 10 K.

($\sim 48 \text{ J mol}^{-1}$) obtained from inelastic neutron scattering studies (Alefeld *et al.*, 1975). The methyl groups are organized in infinite chains with rotational axes parallel to the crystal *c* axis, and the collective rotational dynamics in one dimension has been modelled with the quantum sine-Gordon theory (Fillaux & Carlile, 1990; Fillaux *et al.*, 2003). In the case of 4MPNO, however, the rotational tunnelling spectrum at 4 K is more complicated. There are four transitions, at 81, 111, 192 and 279 μeV , suggesting more hindered rotational dynamics (Carlile *et al.*, 1990; Ikeda *et al.*, 1991). So far, further modelling of methyl-group dynamics has been hampered by the lack of knowledge of the crystal structure at low temperature and it is unknown whether this band manifold arises from different local potentials at crystallographically inequivalent sites or from dynamical coupling.

The structure of 4MPNO has been studied previously at room temperature by single-crystal X-ray (Rose, 1961) and neutron diffraction experiments and was determined to be tetragonal *I*4₁/*amd* with $a = b = 7.964$ (3) and $c = 19.621$ (5) Å (Kaiser, 1997; Kaiser-Morris *et al.*, 1998). Two phase transitions have been reported at 139 and 91 K (Ikeda *et al.*, 1991; Kaiser, 1997). Kaiser (1997) suggested that the intermediate phase could be orthorhombic *Fddd* with $a = 12.01$, $b = 10.46$ and $c = 19.65$ Å, with a reorientation of the molecules around the *c* axis. To the best of our knowledge, the low-temperature phase ($T < 91$ K) of 4MPNO has never been elucidated.

We present here the results of synchrotron and neutron diffraction studies of the fully hydrogenated 4MPNOH and fully deuterated 4MPNOD powders, respectively, in the three crystalline phases. Our results confirm those previously obtained for the phases at high and intermediate temperatures by Kaiser-Morris *et al.* (1998). In addition, we were able to propose a structural model for 4MPNOD at 10 K, which involves a tetragonal cell with space group *P*4₁ [$a = b = 15.410$ (2), $c = 19.680$ (3) Å]. This model gives a good fit to all diffraction data, even though it is impossible to rule out entirely other molecular arrangements. In this model the asymmetric unit contains eight molecules exhibiting a complex pattern of reorientations around the three axes, compared with the intermediate phase. Moreover, in sharp contrast with the simpler structure of 4MP at low temperature, our results evidence localization and ordering of the CD₃ rotors. They suggest two kinds of methyl-methyl interaction: along infinite chains parallel to **a** and **b** on the one

Table 3

Atomic coordinates of the centre of mass and TLS matrix parameters of fully deuterated 4-methylpyridine-*N*-oxide at 250 and 100 K.

The standard uncertainty for the last digit is given in parentheses.

	250 K	100 K
Coordinates of mass centre		
<i>x</i>	0	5/8
<i>y</i>	1/4	1/8
<i>z</i>	0.628 (3)	0.378 (2)
Rotation matrix (°)		
θ	180	180
φ	0	0
χ	90	36.87 (8)
TLS parameters		
t_{11} (Å ²)	0.044 (2)	0.029 (9)
t_{22} (Å ²)	0.062 (1)	0.021 (10)
t_{33} (Å ²)	0.037 (1)	0.014 (5)
l_{33} (rad ²)	0.028 (1)	0.014 (6)
l_{33} (methyl group) (rad ²)	0.76 (16)	0.52 (12)

Table 4

Fractional positions of the centre of mass and orientation (in °, see text) of the eight independent molecules of fully deuterated 4-methylpyridine-*N*-oxide at 10 K, and χ orientation of the corresponding methyl groups.

The standard uncertainty for the last digit is given in parentheses. Note that the standard uncertainty is high for φ and χ because of the high correlation between the two angles when θ is close to 0° (180°).

M1	<i>x</i>	0.654 (2)	θ	−175.7 (6)	M5	<i>x</i>	0.646 (4)	θ	4.5 (6)
	<i>y</i>	0.840 (2)	φ	237 (7)		<i>y</i>	0.586 (4)	φ	14 (6)
	<i>z</i>	0.633 (4)	χ	211 (7)		<i>z</i>	0.378 (2)	χ	−14 (6)
Me1			χ	−76 (8)	Me5			χ	−161 (9)
M2	<i>x</i>	0.904 (4)	θ	173.7 (6)	M6	<i>x</i>	0.666 (4)	θ	−2.4 (7)
	<i>y</i>	0.600 (4)	φ	−47 (5)		<i>y</i>	0.844 (4)	φ	−77 (11)
	<i>z</i>	0.129 (3)	χ	−30 (5)		<i>z</i>	0.134 (3)	χ	143 (11)
Me2	<i>y</i>		χ	−140 (9)	Me6			χ	−258 (16)
M3	<i>x</i>	0.910 (4)	θ	175.8 (6)	M7	<i>x</i>	0.601 (4)	θ	−6.8 (5)
	<i>y</i>	0.849 (4)	φ	−70 (6)		<i>y</i>	0.098 (4)	φ	53 (5)
	<i>z</i>	0.388 (2)	χ	16 (6)		<i>z</i>	0.388 (3)	χ	−27 (5)
Me3			χ	−175 (8)	Me7			χ	−265 (9)
M4	<i>x</i>	0.903 (4)	θ	−4.3 (4)	M8	<i>x</i>	0.650 (4)	θ	176.4 (4)
	<i>y</i>	0.853 (4)	φ	100 (9)		<i>y</i>	0.600 (4)	φ	−15 (11)
	<i>z</i>	0.876 (2)	χ	−94 (9)		<i>z</i>	0.892 (2)	χ	78 (11)
Me4			χ	−212 (14)	Me8			χ	−218 (16)

hand and, on the other, between perpendicular chains through pairs of face-to-face methyl groups along **c**.

2. Experiment

4MPNO is hygroscopic and melts at 463 K. The fully deuterated analogue was obtained by repeated exchanges with heavy water (D₂O). Approximately 0.1 mol of commercial 4MPNO (~10 g) and 0.1 mol of K₂CO₃ (~1.5 g) were dissolved in 10 cm³ of D₂O (99.9%) and held at 253 K for 20 h. The heavy water was then removed under vacuum and this process was repeated three times. ¹H NMR gives deuterium enrichments of 97% at the ring sites and 60% for the methyl groups. After distillation, the partially deuterated sample and 0.01 mol of Na (~0.2 g) were again dissolved in 10 cm³ of D₂O and heated at 263 K for 24 h. The process, repeated twice, gave an enrichment of 97% at all sites. The final yield was 64%.

Synchrotron X-ray diffraction experiments ($\lambda = 0.68964$ Å) were carried out at SNBL-ESRF at 300, 110 and 25 K. The

neutron diffraction study conducted with the high-resolution diffractometer 3T2 ($\lambda = 1.2253$ Å) at LLB (Saclay, France) was carried out on 4MPNOD at 250, 100 and 10 K.

The diffraction patterns were refined using the *FullProf Suite* set of programs (Rodriguez-Carvajal, 1993).¹ The 4MPNOD molecule was represented as a rigid body including the D atoms of the pyridine ring, complemented with a satellite methyl group free to rotate around the C3–C4 bond (one additional degree of freedom). These constraints were necessary for the low-temperature phase, which contains as many as 120 atoms in the asymmetric unit, in order to avoid unrealistic molecular distortions arising from the limited information contained in the powder diffraction pattern. The intramolecular bond lengths and angles were initially calculated from a standard refinement of the structure at 250 K using a planar molecular frame symmetric with respect to its long axis. Apart from the C4–D3 distances and D3–C4–D3

angles, all other distances and angles were kept constant in the refinement processes (Table 1). The calculated distances agree with those found in the parent compounds (Ülkü *et al.*, 1971; Chiang, 1974; Ohms *et al.*, 1985; Carlile & Fillaux, 1990; Vorontsov, 2002; Fillaux *et al.*, 2003), with the N–O distance of 1.39 Å typical of a very limited π -bond character (Ülkü *et al.*, 1971). The molecular thermal motions of the rigid body and of the satellite methyl group were refined by means of the appropriate molecular displacement tensors, the TLS matrices (Schomaker & Trueblood, 1968).

3. Results and discussion

3.1. 250 K structure

The structural refinement of the neutron powder diffraction data collected at 250 K (Fig. 2) confirms that 4MPNOD is tetragonal (*I4₁/amd*) with cell parameters $a = b = 7.941$ (3) and $c = 19.600$ (5) Å (Fig. 3; Kaiser, 1997; Kaiser-Morris *et al.*, 1998). The structure contains eight equivalent molecules per unit cell, the molecular site symmetry being *2mm*. The molecular long axes are alternatively oriented along **c** and the molecular planes are parallel to (100) or (010). Structural parameters are gathered in Tables 2 and 3.² The CD₃ satellite group libration parameter, $l_{33} = 0.76$ (16) rad², yields reasonably good agreement factors for the refinement. This value is compatible with an almost isotropic distribution around the C3–C4 bond (Fig. 4). Furthermore, Fourier maps of the D-atom distribution in the rotational plane confirm that both standard and rigid-body refinements lead to a circular density

¹ *FullProf_Suite* can be downloaded from <ftp://ftp.cea.fr/pub/llb/divers/fullprof.2k>.

² Supplementary data for this paper are available from the IUCr electronic archives (Reference: AV5052). Services for accessing these data are described at the back of the journal.

(Fig. 4), very similar to that of 4MP at 260 K (Fillaux *et al.*, 2003).

3.2. 100 K structure

The neutron data at 100 K (Fig. 2) confirm the orthorhombic phase with the *Fddd* space group deduced from a powder X-ray diffraction study by Kaiser (1997), with cell parameters $a = 12.138$ (2), $b = 10.237$, $c = 19.568$ (3) Å (Table 2). The unit cell contains 16 equivalent molecules with their long axes parallel to **c**, but the molecular plane is now tilted by $\sim 36.9^\circ$ (Fig. 3, Table 3) with respect to **a** or **b**. The molecular site symmetry is 2, which implies a disordered methyl group as in the 250 K structure. Compared with the structure at 250 K, where consecutive molecules along the *c* axis are perpendicular to each other, the angle of $\sim 73.8^\circ$ at 100 K is equivalent to a rotation of the molecular planes by $\sim 8.1^\circ$ around the *c* axis. Lengthening the C4–D3 distances in the molecule rigid body leads to significant improvement of the refinement (Table 1). Fourier maps still show rotational disordering (Fig. 4). The square-like distribution is similar to that reported by Kaiser-Morris *et al.* (1997) for the hydrogenated single crystal at 160 K. This distribution can be rationalized with either coupled rotational and translational motions of the methyl groups (Schiebel *et al.*, 1998) or convolution of the probability density distributions of the disordered methyl groups and of the orientation of the C3–C4 rotational axis (Nicolai *et al.*, 2003). These models cannot normally be distinguished in diffraction experiments.

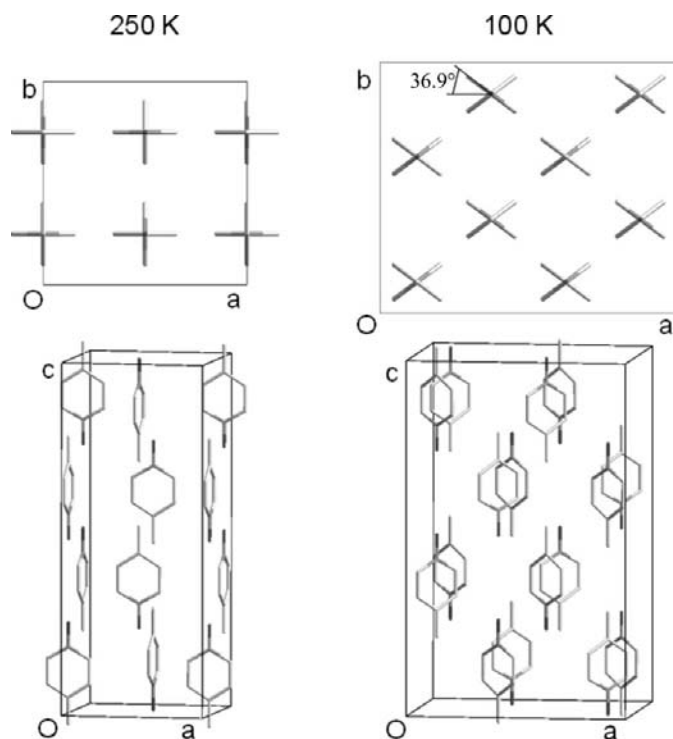


Figure 3
[001] projection and unit cell of the structure of 4-methylpyridine-N-oxide at 250 and 100 K. For the sake of clarity the D atoms are omitted.

3.3. 10 K structure

In order to investigate the possible cell parameters and lattice symmetries at 10 K, the indexing program *DicVol* (Boultif & Louër, 1991) included in the *FullProf Suite* (Rodriguez-Carvajal, 1993) was first applied to the synchrotron data collected for the fully hydrogenated 4MPNOH at 25 K. The program converged to a reliable solution, that is, a tetragonal cell with $a = b = 15.454$ and $c = 19.695$ Å, which approximately corresponds to a doubling along the *a* and *b* directions of the cell at 250 K. Simulated annealing (Rodriguez-Carvajal, 1993) using clusters of integrated intensities was subsequently applied to test different space groups amongst the subgroups of $I4_1/amd$, compatible with the

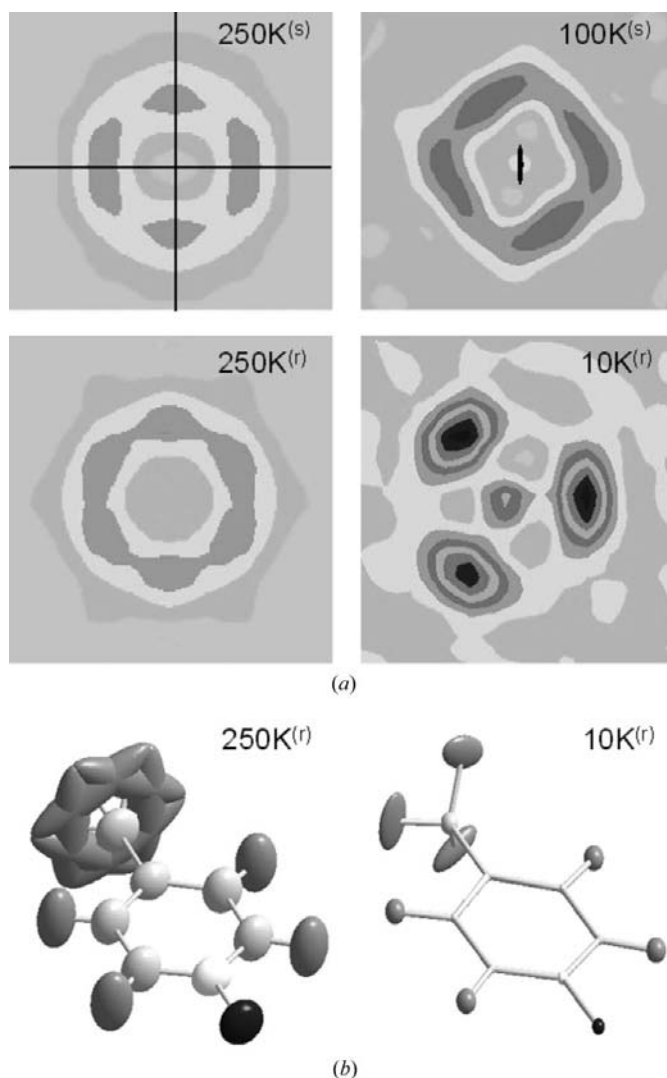


Figure 4
(a) Isodensity contours (Fourier method) in the rotational plane (001) of the deuterated methyl group at 250, 100 and 10 K. Superscripts (s) and (r) refer to standard and rigid-body group refinements, respectively. Symmetry elements are shown for 250 K^(s) (mirrors) and 100 K^(s) (twofold axis). (b) Schematic views of the molecules and displacement ellipsoids at 250 K (illustrating the modelling of the orientational disordering of the deuterated methyl group), and at 10 K (shown is molecule M8).

transformation matrix [200/020/001]. Rigid-body molecules were positioned according to the structure at 250 K. Positions (x, y, z) and rotations were defined by Euler angles θ, φ and χ in such a way that if (X_o, Y_o, Z_o) refers to the orthonormal cell system and (X_m, Y_m, Z_m) to the rigid-body internal system, φ corresponds to a rotation of the (X_m, Y_m, Z_m) system around

Z_o , θ corresponds to the angle between Z_o and Z_m , and χ corresponds to a rotation around Z_m . It is important to note that in order for the simulated annealing algorithm to converge towards a solution, the positions of the molecules' centres of mass had to be framed into a 1.0 Å-side square box, so as to avoid unlikely molecular motions. Similarly, the θ

rotation of the (X_m, Y_m, Z_m) system was limited to a maximum of 45° with respect to the 250 K structure. No restriction was imposed on the φ and χ rotations.

The cell containing eight independent molecules ($Z = 32$) in the $P4_1$ space group gave the only convergent solution and was therefore selected for the refinement of the 10 K neutron diffraction pattern (Fig. 2) as the most probable model. The cell parameters, positions and rotations of the eight rigid-body molecules were refined, including the rotational angle χ of the satellite groups. Isotropic displacement parameters were applied to all atoms except the methyl groups, for which a common TLS matrix was used. The final refinement (bottom of Fig. 5, Table 2) is very satisfactory, considering the heavy constraints of the rigid-body model. The 'true' intramolecular distances and angles at low temperature should be close to those of the rigid-body model, and variations between crystallographically distinct molecules are probably insignificant. It turns out that synchrotron data for 4MPNOH (top of Fig. 5) and neutron data for 4MPNOD lead to similar structures. To further confirm the $P4_1$ space group, automatic searches for missed symmetry elements in the structure were carried out but systematically failed. NMR studies on this compound could prove a valuable complementary tool to validate the number of crystallographically independent molecules; in addition, the preliminary results of a neutron diffraction study on single crystals of 4MPNOD carried out in our laboratory agree with the $P4_1$ model.

The structure at 10 K is illustrated in Fig. 6. Reorientations

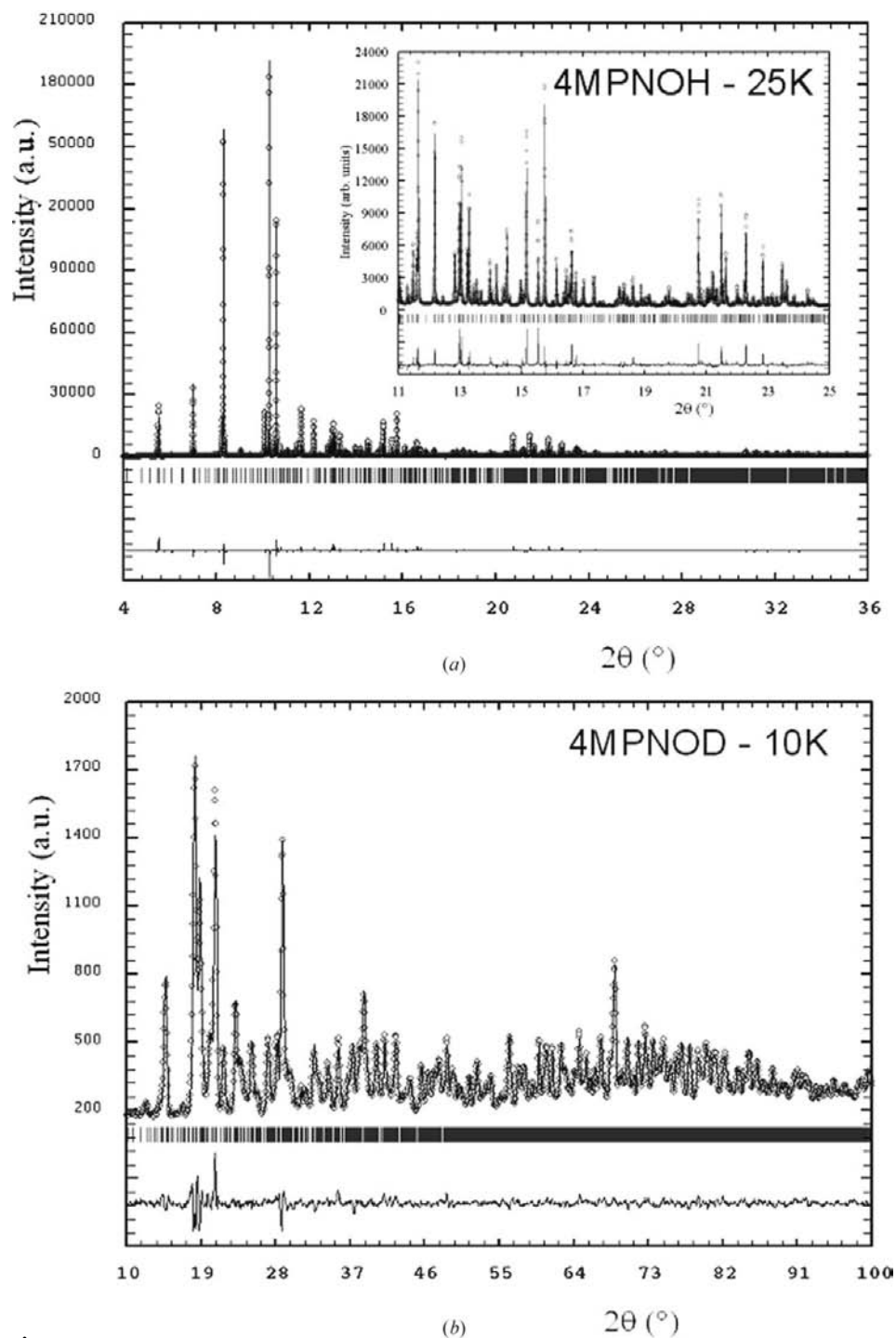


Figure 5 Rietveld refinement of the synchrotron (upper panel) and neutron (lower panel) diffraction patterns of fully hydrogenated and deuterated 4-methylpyridine-*N*-oxide at 25 and 10 K, respectively. Experimental data: open circles; calculated: continuous line; allowed Bragg reflections: vertical marks. The difference between the observed and calculated profiles is displayed at the bottom. The inset of the upper panel shows an enlargement of the synchrotron data refinement at high angles.

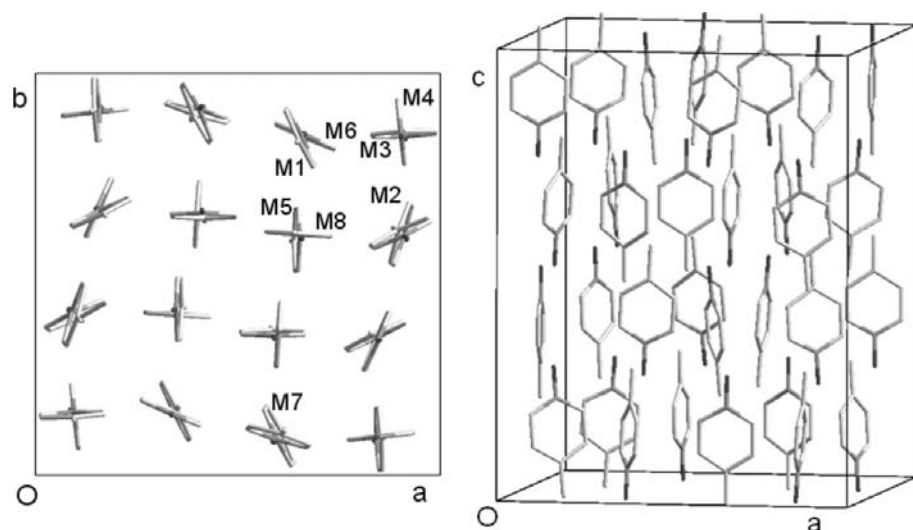


Figure 6
[001] projection of the unit cell for fully deuterated 4-methylpyridine-*N*-oxide at 10 K. The D atoms are omitted. M1–M8 refer to the eight molecules of the asymmetric unit defined in Table 4.

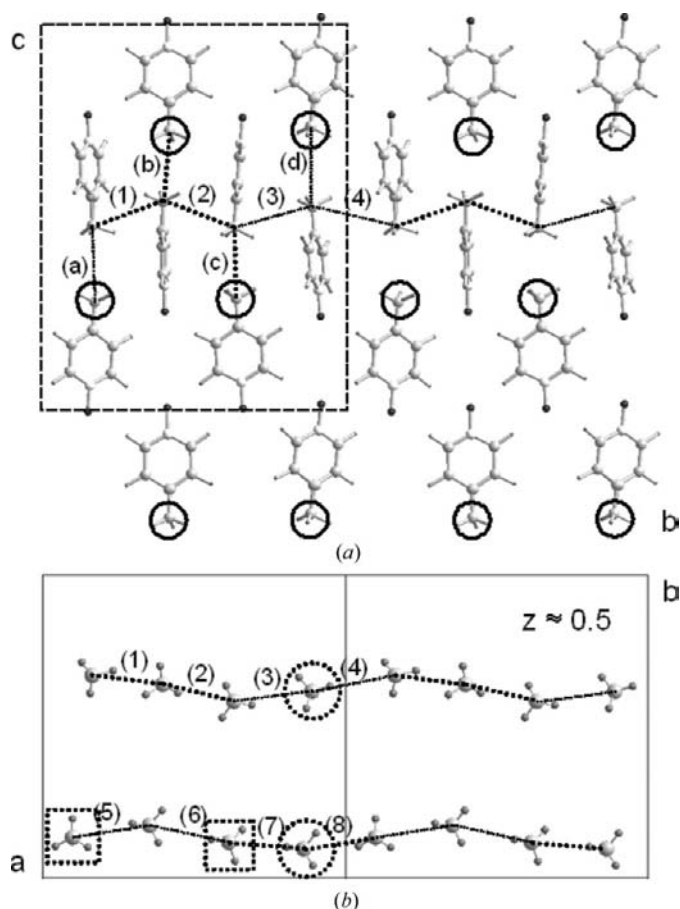


Figure 7
(a) View along **a** of the infinite chains of CD₃ rotors parallel to **b** (zigzag lines) or parallel to **a** (circles). The unit cell is outlined. (b) View along **c** of two chains. Numbers in parentheses refer to the distances between methyl groups in Table 5. Thick and thin dots correspond to short and long distances, respectively. Dotted circles emphasize possible coupling with rotors in the next layer ($z \approx 0.7$) above, while dotted squares indicate possible coupling with rotors in the next layer ($z \approx 0.3$) below.

around **a**, **b** and **c** of the eight different molecules during the phase transition are rather complex (Table 4). Along **c**, two columns of roughly perpendicular molecules alternate with two columns of molecules tilted by about 40°. This pattern is actually reminiscent of a combination of the structures at 250 and 100 K, respectively. The molecular site symmetry in $P4_1$ is 1 and the displacement ellipsoids calculated from the TLS matrix show that the methyl groups are now largely localized (Fig. 4, Table 5). This is also clearly demonstrated by the Fourier maps at 10 K (Fig. 4).

The manifold of tunnelling transitions observed for 4MPNO could be related to different crystallographic sites for methyl groups. Since the four tunnelling bands have similar intensities, and since there are eight crystal-

lographically independent methyl groups, each band should be twofold degenerate. A more detailed assignment scheme is, however, beyond the scope of this work.

Compared with 4MP, the longest axis of the 4MPNO molecule is increased by 1.39 Å, while the *c* lattice parameter, along which four molecules are stacked, is increased by only 1.2 Å. Consequently, the rather short distances between O and methyl groups may contribute to the increase of the rotational barrier in 4MPNO and favour orientational ordering at low temperature.

On the basis of distances between methyl groups, one can distinguish face-to-face pairs and infinite chains in 4MPNO (Fig. 7), much in the same way as for 4MP. The distances between face-to-face methyl groups along **c** [distances (a) to (d) ranging from 3.62 to 4.09 Å see Fig. 7 and Table 5] are significantly longer than the distance of 3.462 Å for 4MP. However, the fourfold axis for methyl pairs in 4MP automatically destroys any orientational correlation and disordering survives at low temperature. By contrast, the lack of symmetry for face-to-face pairs in 4MPNO permits orientational correlation despite the longer methyl–methyl distances, and possibly weaker interaction. In fact, the structure suggests that half of the face-to-face methyl groups are in phase (dotted circles and squares on the bottom panel of Fig. 7), while the remaining CD₃ groups are in random positions.

The arrangement of methyl chains in 4MPNOD is quite different from that in 4MP. The two sets of slightly distorted orthogonal infinite chains are nearly parallel to **a** and **b** (circles and zigzag dotted lines, respectively, in Fig. 7). The distances along such chains, namely (1) to (4) and (5) to (8) in Fig. 7 and Table 5, range from 3.80 to 4.41 Å, and from 3.92 to 4.22 Å. Two short distances alternate with two long ones along chains. Compared with 4MP, the translational invariance of the methyl groups is destroyed. A detailed analysis suggests that methyl groups within a chain are ordered in phase, one chain being anti-phase with respect to the next parallel one (Fig. 7).

Table 5

Intermolecular distances in fully deuterated 4-methylpyridine-*N*-oxide at 10 K (Fig. 7) and TLS matrix parameters.

The standard uncertainty for the last digit is given in parentheses.

(1)	3.799 (4)	(7)	3.956 (4)
(2)	3.948 (4)	(8)	3.918 (4)
(3)	4.147 (4)	(a)	3.914 (4)
(4)	4.408 (6)	(b)	3.625 (4)
(5)	4.139 (4)	(c)	3.625 (4)
(6)	4.219 (4)	(d)	4.087 (4)
t_{11} (Å ²)	0.019 (5)	t_{33} (Å ²)	0.023 (5)
t_{22} (Å ²)	0.050 (7)	l_{33} (rad ²)	0.071 (6)

Direct interaction between parallel chains that are more than 7 Å apart is negligible.

4. Conclusion

The neutron diffraction data of powdered deuterated 4MPNOD at 250, 100 and 10 K, combined with the X-ray diffraction data for the hydrogenated analogue, allowed us to elucidate the three different phases of this compound. At 10 K our model shows the existence of eight distinct molecular sites, which suggests that the four tunnelling transitions observed with inelastic neutron scattering could correspond to different effective potentials for methyl rotors. Compared with the parent system 4MP, the fourfold symmetry for methyl pairs and the translational invariance of the methyl sites are destroyed. As a consequence, unlike 4MP, rotational dynamics in 4MPNO cannot be described by the quantum sine-Gordon model in one-dimension.

The authors are indebted to N. Leygue from LADIR for sample preparation.

References

- Alefeld, B., Kollmar, A. & Dasannacharya, B. A. (1975). *J. Chem. Phys.* **63**, 4415–4417.
- Boultif, A. & Louër, D. (1991). *J. Appl. Cryst.* **24**, 987–993.
- Carlile, C. J. & Fillaux, F. (1990). ISIS Experimental Report RB 1090. ISIS, Chilton, Didcot OX11 0DG, UK.
- Carlile, C. J., Willis, B. T. M., Ibberson, R. M. & Fillaux, F. (1990). *Z. Kristallogr.* **193**, 243–250.
- Chiang, J. F. (1974). *J. Chem. Phys.* **61**, 1280–1283.
- Fillaux, F. & Carlile, C. J. (1990). *Phys. Rev. B*, **42**, 5990–6006.
- Fillaux, F., Nicolai, B., Paulus, W., Kaiser-Morris, E. & Cousson, A. (2003). *Phys. Rev. B*, **68**, 224301-1–13.
- Ikeda, S., Watanabe, N., Inoue, K., Kiyonagi, Y., Inaba, A., Takeda, S., Kanaya, T., Shibata, K., Kamiyama, T., Izumi, Y., Ozaki, Y. & Carlile, C. J. (1991). *J. Phys. Soc. Jpn.* **60**, 3340–3350.
- Kaiser, E. (1997). PhD thesis, Laboratoire Léon Brillouin, France.
- Kaiser-Morris, E., Cousson, A. & Paulus, W. (1998). *Z. Kristallogr.* **213**, 80–80.
- Kaiser-Morris, E., Paulus, W., Cousson, A., Heger, G. & Fillaux, F. (1997). *Physica B*, **234–236**, 74–75.
- Nicolai, B., Cousson, A. & Fillaux, F. (2003). *Chem. Phys.* **290**, 101–120.
- Ohms, U., Guth, H., Treutmann, W., Dannohl, H., Schweig, A. & Heger, G. (1985). *J. Chem. Phys.* **83**, 273–279.
- Rodriguez-Carvajal, J. (1993). *Physica B*, **192**, 55–69.
- Rose, H. A. (1961). *Acta Cryst.* **14**, 895–895.
- Schiebel, P., Kearley, G. J. & Johnson, M. R. (1998). *J. Chem. Phys.* **108**, 2375–2382.
- Schomaker, V. & Trueblood, K. N. (1968). *Acta Cryst.* **B24**, 63–76.
- Ülkü, D., Huddle, B. P. & Morrow, J. C. (1971). *Acta Cryst.* **B27**, 432–436.
- Vorontsov, I. I. (2002). *J. Mol. Struct.* **610**, 271–276.